

Inferring Semantic Information with 3D Neural Scene Representations

Amit Kohli*, Vincent Sitzmann*, and Gordon Wetzstein

Stanford University

{apsk14, sitzmann, gordon.wetzstein}@stanford.edu

Abstract. Biological vision infers multi-modal 3D representations that support reasoning about scene properties such as materials, appearance, affordance, and semantics in 3D. These rich representations enable us humans, for example, to acquire new skills—such as the learning of a new semantic class—with extremely limited supervision. Motivated by this ability of biological vision, we demonstrate that 3D-structure-aware representation learning leads to multi-modal representations that enable 3D semantic segmentation with extremely limited, 2D-only supervision. Building on emerging neural scene representations, which have been developed for modeling the shape and appearance of 3D scenes supervised exclusively by posed 2D images, we are first to demonstrate a representation that jointly encodes shape, appearance, and semantics in a 3D-structure-aware manner. Surprisingly, we find that only a few tens of labeled 2D segmentation masks are required to achieve dense 3D semantic segmentation using a semi-supervised learning strategy. We explore two novel applications for our semantically aware neural scene representation: 3D novel view and semantic label synthesis given only a single input RGB image or 2D label mask, as well as 3D interpolation of appearance and semantics.

1 Introduction

Representations of 3D objects learned by humans are multi-modal and support learning of new information with extremely limited supervision. For instance, a person does not need to be told that a car wheel is a car wheel thousands of times, but only a few tens of times. Subsequently, this newly learned semantic label can be directed associated with the person’s mental image of a car. In addition, representations learned by humans enable 3D semantic reasoning: Observing a single side-view picture of a car, humans can easily imagine what the other side of the car will look like, including the different semantic classes of the parts involved, such as car door, wheel, or car window.

A similar level of semi-supervised learning and 3D scene understanding is also crucial for many tasks in computer vision, robotics, and autonomous driving. In these applications, algorithms must reason about a 3D scene given only partial information, such as a single image. In robotic grasping, for instance, a robot has to simultaneously reason about the 3D geometry, appearance, and semantic

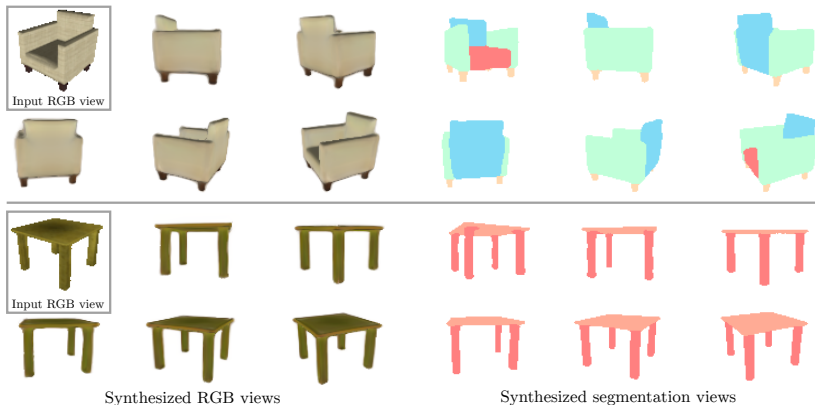


Fig. 1. We leverage 3D-structure-aware representation learning for 3D reconstruction and semantic segmentation of objects, jointly reasoning about shape, appearance, and semantics. In this particular application, a single RGB image of an unseen object (upper left) is fed into the network, which is then capable of synthesizing perspective-consistent 3D RGB views of the object (left) as well as part-level semantic segmentation labels (right).

structure of an object in order to choose the optimal grasping point. In addition, human labeling is expensive, and these applications would thus greatly benefit from label-efficient learning approaches.

Recent progress in representation learning has enabled competitive performance on 2D tasks when only a limited amount of training data is available [78,4,23,2,13]. Here, 2D feature extractors are trained with massive amounts of unlabeled data on a surrogate task. Once the representation is learned, a limited amount of training data can be sufficient to train a simple classifier on the pre-trained feature representation [23]. While these approaches are applicable to 2D, image-based problems, they do not build a 3D-aware representation. Given a single image observation, they are incapable of making predictions about unseen perspectives of the scene or occluded parts, a task that is critical to 3D scene understanding and interaction.

Concurrently, 3D neural scene representations are an emerging paradigm to tackle problems in inverse graphics and 3D computer vision [60,14,15,71,75,63,31,38,58,56]. Given 2D image observations, these approaches aim to infer a 3D-structure-aware representation of the underlying scene that enables prior-based predictions about occluded parts. These scene representations have thus far been primarily explored for applications in view synthesis, but not for scene understanding. A naïve approach would be to generate arbitrary perspectives of a scene from limited observations and then apply standard 2D methods for semantic segmentation or other tasks. Such image-based approaches, however, fail to infer a

compact, multi-modal representation that would allow for joint reasoning about *all* aspects of the scene.

Here, we propose to use neural scene representations not for view synthesis, but as a representation learning backbone, enabling downstream tasks by inferring a multi-modal, compact 3D representation of objects from 2D images. Our work adopts continuous scene representation networks enabling, for the first time, dense 3D semantic segmentation given only 2D observations. We then embed the latent 3D feature representation, learned in an unsupervised manner given only posed 2D RGB images, in a standard semi-supervised learning strategy for semantic segmentation. This enables dense 3D semantic segmentation given extremely limited labeled training data of just a few tens of semantic segmentation labels. We demonstrate that this unique combination of unsupervised, 3D-structure-aware pre-training and supervised fine-tuning enables multi-view consistent view synthesis and semantic segmentation (see Fig. 1). Our approach further enables several other novel applications, including interpolation of 3D segmentation labels as well as 3D view and semantic label synthesis from just a single observed image or semantic mask. To summarize, we make the following key contributions:

- We extend scene representation networks to perform semantic segmentation, leading to a semantically and 3D-structure-aware neural scene representation.
- In a semi-supervised learning framework, we demonstrate that the resulting representation can be leveraged to perform dense 3D semantic segmentation from only 2D observations, given as few as 30 semantic segmentation masks. We demonstrate that features learned by the 3D neural scene representation far outperform a neural scene representation without 3D structure.
- We demonstrate multi-view consistent rendering of semantic segmentation masks, including parts of the object that are occluded in the observation.
- We demonstrate joint interpolation of geometry, appearance, and semantic labels, and demonstrate how a neural scene representation can be inferred from either a color image or a semantic segmentation mask.

2 Related Work

Inferring properties of 3D environments given limited amounts of labeled training data has been a long-standing challenge in the computer vision community. Our approach takes a step towards this goal by combining insights from representation learning, neural scene representations, and 3D computer vision. Each of these fields builds on extensive literature, which we summarize as follows.

3D Computer Vision Deep-learning-based models for geometry reconstruction were among the first to propose 3D-structured latent spaces to enable 3D reasoning about scenes. Discretization-based techniques use voxel grids [29,64,69,18,50,59,26,6], octree hierarchies [53,62,22], point clouds [48,1,61], multiplane images [76], patches

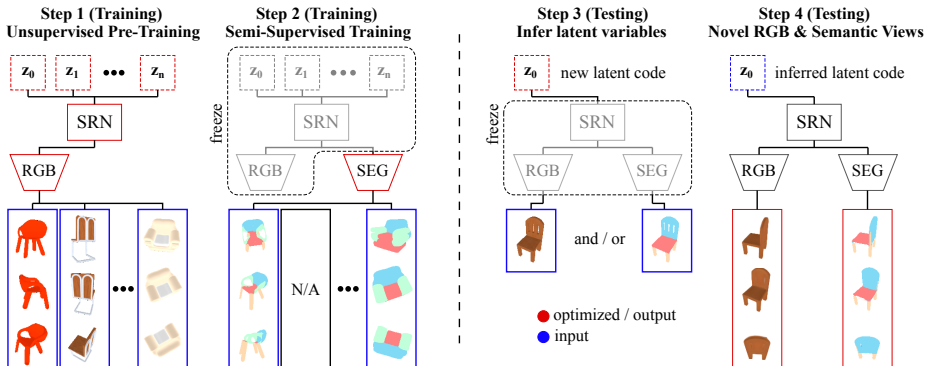


Fig. 2. Overview of the proposed semi-supervised method. From left to right: (1) We train a scene representation network (SRN) for novel view synthesis of RGB images using a large dataset of 2D posed images in an autoencoder-framework [46], where each object instance is represented by its own code vector z_i . (2) We then freeze code vectors and weights of the SRN and train a linear segmentation classifier on SRN features, using human-annotated semantic labels of a *very small* (30 images) subset of object instances in the training set. (3) At test time, given a *single* posed RGB image and/or label mask of an instance unseen at training time, we infer the latent code of the novel object. (4) Subsequently, we may render multi-view consistent novel RGB and semantic segmentation views of the object instance.

[20], or meshes [25,26,30,28]. Methods based on function spaces continuously represent space as the decision boundary of a learned binary classifier [37] or a continuous signed distance field [46,19,10]. While these methods model the underlying 3D geometry of a scene, they do not model aspects of the scene other than geometry.

2D Representation Learning A large body of work explores self-supervised representation learning on images [13,23,2,27,32,52,9,11,73,43,34,70,12,51,44]. These approaches have yielded impressive results on 2D tasks such as bounding box detection, 2D image segmentation, and image classification. However, none of these approaches builds a 3D-structure-aware representation. This lack of 3D inductive bias makes these approaches incapable of reasoning about multi-view consistency or objects parts occluded in the input image. Fundamentally, 2D representation learning is therefore incapable of supporting 3D semantic labeling from 2D input.

Neural Scene Representations A recent line of work reconstructs both appearance and geometry given only 2D images and their extrinsic and intrinsic camera parameters. Auto-encoder-like methods only weakly model the latent 3D structure of a scene [60,68]. Generative Query Networks [16,33] introduce a probabilistic reasoning framework that models uncertainty due to incomplete observations, but both the scene representation and the renderer are oblivious to the

scene’s 3D structure. Some recent work explores voxel grids as a scene representation [55,65,42,77,41]. Our approach builds on recent continuous, 3D-structure-aware scene representations [45,57]. Using standard semi-supervised learning techniques, we demonstrate that scene representation networks (SRNs) [57] in particular enable us to infer 3D semantic labels given only a single 2D image observation, trained with very limited amounts of labeled data. Although differentiable continuous functions have been explored for 3D shape and appearance representation in the past, we are the first to explore their application to 3D-structure-aware scene segmentation.

Semantic Segmentation The advent of deep learning has had a transformative impact on the field of semantic segmentation. Seminal work by Long et al. [36] introduced fully convolutional neural networks for pixel-level semantic labeling. Numerous CNN-based approaches further refined this initial idea [5,74,72,54]. Recent work in this area has increasingly incorporated ideas from 3D computer vision. Semantic segmentation has thus been formulated in cases where both geometry and color information are available [7,66,67]. However, these methods operate on point clouds or voxel grids and therefore rely on explicit geometry representations. To the best of our knowledge, no semantic segmentation approach infers 3D semantic labels given a 2D RGB image, which our approach enables. Note that we do *not* claim performance gains on 2D semantic segmentation. Our goal is to learn a single representation that jointly encodes information about 3D geometry, appearance and semantic segmentation. While we do rely on comparisons in image space, as this is the only data we have access to, we stress that this is merely a surrogate to demonstrate that the 3D representation contains semantic information, and not an attempt at an incremental improvement on 2D semantic segmentation.

3 Method

In the following section, we first review scene representation networks (SRNs) [57]. We then demonstrate how we can extend SRNs to perform 3D semantic segmentation by adding a *Segmentation Renderer* in parallel to the existing *RGB Renderer*. Finally, we view SRNs through the lense of representation learning and apply a semi-supervised learning strategy. This yields 3D semantic segmentation from 2D RGB observations and their camera parameters, given an extremely limited number of semantic segmentation masks.

3.1 Scene Representation Networks (SRNs)

Scene Representation Networks are a continuous, 3D-structure aware neural scene representation. They enable reconstruction of 3D appearance and geometry, trained end-to-end from only 2D images and their camera poses, without access to depth or shape. The key idea of SRNs is to encode a scene in the weights $\mathbf{w} \in \mathbb{R}^l$ of a fully connected neural network, the SRN itself. To this end,

a scene is modeled as a function that maps world coordinates \mathbf{x} to a feature representation of local scene properties \mathbf{v} :

$$\text{SRN} : \mathbb{R}^3 \rightarrow \mathbb{R}^n, \quad \mathbf{x} \mapsto \text{SRN}(\mathbf{x}) = \mathbf{v}. \quad (1)$$

Images are synthesized from this 3D representation via a differentiable neural renderer consisting of two parts. The first is a differentiable ray marcher which finds intersections of camera rays with scene geometry by marching along a ray away from a camera. At every step, it queries SRN at the current world coordinates and translates the resulting feature vector into a step length. Finally, SRN is queried a final time at the regressed ray intersection points, and the resulting feature vector \mathbf{v} is mapped to an RGB color via a fully connected neural network, which we refer to as the *RGB Renderer*. Due to the differentiable rendering, SRNs may be trained given only 2D camera images as well as their intrinsic and extrinsic camera parameters.

To generalize across a class of objects, it is assumed that the weights \mathbf{w}_j of SRNs that represent object instances within the same class lie in a low-dimensional subspace of \mathbb{R}^l , permitting us to represent each object via an embedding vector $\mathbf{z}_j \in \mathbb{R}^k$, $k < l$. A hypernetwork [21] HN maps embedding vectors \mathbf{z}_j to the weights \mathbf{w}_j of the respective scene representation network:

$$\text{HN} : \mathbb{R}^k \rightarrow \mathbb{R}^l, \quad \mathbf{z}_j \mapsto \text{HN}(\mathbf{z}_j) = \mathbf{w}_j. \quad (2)$$

HN thus learns a prior over the weights of scene representation networks and thereby over scene properties. To infer the scene representation of a new scene or object, an embedding vector \mathbf{z} is randomly initialized, the weights of HN and the differentiable rendering are frozen, and \mathbf{z} is optimized to obtain a new scene embedding via minimizing image reconstruction error.

3.2 Semantically-aware Scene Representation Networks

We extend the SRN framework to perform joint 3D reconstruction and semantic segmentation. We formalize semantic segmentation as a function that maps a world coordinate \mathbf{x} to a distribution over semantic labels \mathbf{y} . This can be seen as a generalization of point cloud- and voxel-grid-based semantic segmentation approaches [8,47,49], which label a discrete set of world coordinates, sparsely sampling an underlying, continuous function. To leverage SRNs for semantic segmentation, we represent the semantic label function as a composition of the scene representation network (eq. 1) and an additional *Segmentation Renderer* SEG that maps a feature vector \mathbf{v} to a distribution over class labels \mathbf{y} :

$$\text{SEG} : \mathbb{R}^n \rightarrow \mathbb{R}^m, \quad \mathbf{v} \mapsto \text{SEG}(\mathbf{v}) = \mathbf{y}. \quad (3)$$

In other words, this amounts to adding a *Segmentation Renderer* in parallel to the existing *RGB Renderer*. We may now enforce a per-pixel cross-entropy loss on the output of SEG at any world coordinate \mathbf{x} :

$$\mathcal{L}_{\text{co}} = \sum_{j=1}^c \hat{y}_j \log \sigma(\text{SEG}(\text{SRN}(\mathbf{x}))) \quad (4)$$

where \hat{y}_j is a one-hot ground-truth class label with c number of classes, and σ is the softmax function. The segmentation renderer can be trained end-to-end with the classic SRN architecture. In effect, this supervises the features \mathbf{v} encoded in SRN to carry information about geometry via the ray-marcher, RGB color via the *RGB Renderer*, and semantic information via the *Segmentation Renderer* SEG. At test time, this formulation allows us to infer a code vector \mathbf{z} from either RGB information, semantic segmentation information, or both. In any of these cases, a new code vector is inferred by freezing all network weights, initializing a new code vector \mathbf{z} , and optimizing \mathbf{z} to minimize image reconstruction and/or cross entropy losses, see Fig. 2, Step 3.

3.3 Semi-Supervised Learning of Semantically-aware SRNs

While training an SRN end-to-end with a segmentation renderer on a large dataset of human-labeled images is intuitive, it has a significant weakness: it relies on a massive amount of labeled semantic data. Such labeled data may be difficult to obtain for a variety of different computer vision tasks. Moreover, it is desirable for an independent agent to infer an understanding of the different modes of an object it has not encountered. Such an unsupervised exploration cannot rely on a pipeline that requires thousands or millions of interactions with each object class to infer semantic properties.

For computer vision models that operate on per-pixel features, such as image recognition, object bounding box detection, or 2D semantic segmentation, the emerging field of *representation learning* aims to address this problem [4,23,2,13]. However, none of these approaches infer a 3D-aware representation that would support predictions about parts of an object that are occluded in the input image.

Inspired by these approaches, we interpret SRNs as a representation learning technique. The multi-view re-rendering loss at training time can be seen as enforcing that the underlying representation, SRN, encodes information about appearance and geometry. We hypothesize that features that encode appearance and geometry will also be useful for the downstream task of dense 3D semantic segmentation.

We assume that for a small subset of our training corpus of RGB images and their camera parameters, we are given a few human-labeled per-pixel semantic labels. We now embed SRNs in a standard semi-supervised training framework. Fig. 2 summarizes the proposed semi-supervised approach. In the first step, we pre-train the weights of the hypernetwork HN, the latent embeddings \mathbf{z}_i of the object instances in the training set, as well as the weights of the differentiable rendering purely for image reconstruction requiring only posed RGB images as well as their extrinsic and intrinsic camera parameters. Subsequently, we freeze \mathbf{z}_i as well as the weights of HN and the differentiable renderer and train the proposed *Segmentation Renderer* SEG on the learned feature vectors \mathbf{v} , supervised with human-labeled semantic segmentation masks of a small subset of the training images. In this case of limited training data, we choose to parameterize the segmentation renderer SEG as a simple linear classifier.

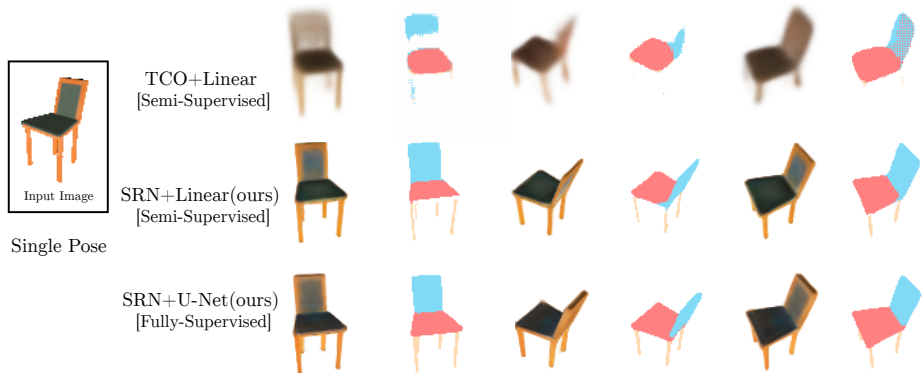


Fig. 3. Comparison of the *single view* models, which can synthesize arbitrary RGB and segmentation views from a single posed RGB image. The proposed semi-supervised *SRN+linear* qualitatively outperforms the baseline semi-supervised approach by Tatarchenko et al. [60] (TCO) and is comparable to the fully-supervised *SRN+U-Net* approach in terms of 3D consistency and semantic segmentation. Note that all other models, including the *Oracle RGB+U-Net*, cannot perform such a task and require all views of ground truth RGB images at test time in order to perform segmentation.

4 Analysis

In this section, we demonstrate that the proposed representation learning approach using 3D-structure-aware neural scene representations succeeds in dense 3D semantic segmentation given extremely few labels. Model code and datasets will be made publicly available upon publication.

Note that we do *not* claim performance gains on existing 2D semantic segmentation approaches. Instead, our goal is to learn a single, compact representation that jointly encodes information about 3D geometry, appearance and semantic segmentation. To do so, we have to rely on comparisons in image space, as this is the only data we have access to. We stress that this is merely a surrogate to demonstrate that the 3D representation contains semantic information, and not an attempt at an incremental improvement on 2D semantic segmentation. Note that existing 2D representation learning techniques are *not* applicable to the problem at hand, as they do not infer a 3D-aware representation and therefore rely on image input that shows all the parts of an object for which features are to be extracted. While it is possible to achieve similar input-output behavior with 2D approaches by building a pipeline that first leverages SRNs for novel view synthesis and subsequently feeds the image to a 2D model, this does *not* demonstrate a multi-modal 3D representation, but rather encodes 3D information in the SRNs representation and semantic information in the 2D architecture. This doesn't support simultaneous reasoning about multiple modalities in 3D, which is critical to many real-world computer vision tasks. We thus refrain from comparisons to such baselines.

Implementation. We implement all models in PyTorch. We train SRN-based models on Nvidia RTX8000 GPUs, and other models on Pascal TitanX GPUs. The SRN as well as the *RGB Renderer* are implemented as 4-layer MLPs with 256 units each, ReLU nonlinearities, and LayerNorm before each nonlinearity. The raymarcher is implemented as an LSTM [24] with 256 units. We ray march for 10 steps. We train our models using ADAM with a learning rate of $4e-4$. SRN-based models are trained for 20k steps at a resolution of 64 with a batch size of 92, and trained for another 85k steps at a resolution of 128 with a batch size of 16. Image reconstruction loss and cross-entropy loss are weighted 200 : 8, such that their magnitudes are approximately equal.

Dataset. For all experiments, we use the PartNet [39] and ShapeNet [3] datasets, which contains 3D meshes as well as their human-labeled semantic segmentation for a variety of object classes. We conduct experiments using the chairs and tables classes, with 4489 and 5660 object instances in the training set, 617 and 839 in the validation set, and 1214 and 1656 in the test set respectively. Partnet contains labels at several resolutions. We conduct all experiments at the coarsest level of segmentation, leading to 6 and 11 semantic classes respectively. We render observations using the Blender internal rasterizer. For training and validation sets, we render 50 camera perspectives sampled at random on a sphere around each object instance. For the test set, we render 251 camera perspectives sampled from an Archimedean spiral around each object instance. All datasets will be made publicly available upon publication.

Evaluation. For quantitative evaluation of segmentation accuracy in image space, we adopt the mean pixel intersection over union (mIOU) and shape mIOU metric. We compute mIOU over all classes including the background class. For a single image, mIOU averages intersection over union over all classes. We subsequently compute the mean of mIOUs over all images and instances. In contrast, shape mIOU averages intersection over union scores across all images and instances separately for each semantic class. Note that the shape mIOU score is generally much lower than the mIOU score. This is due to the fact that the chosen objects have rare semantic classes that appear only in a small subset of all instances and are thus very difficult to score well on, lowering the per class average of shape mIOU.

4.1 Representation learning for semi-supervised semantic segmentation.

We experimentally evaluate the proposed multi-modal, 3D-aware neural scene representation. We show how this enables dense 3D semantic segmentation from extremely few labels, given only *a single 2D observation of an object*, supporting subsequent multi-view consistent rendering of semantic information.

As discussed in 3.3, we first pre-train one scene representation network per object class to obtain a 3D-structure-aware neural scene representation. We then pseudo-randomly sample 10 object instances from the training set such that all

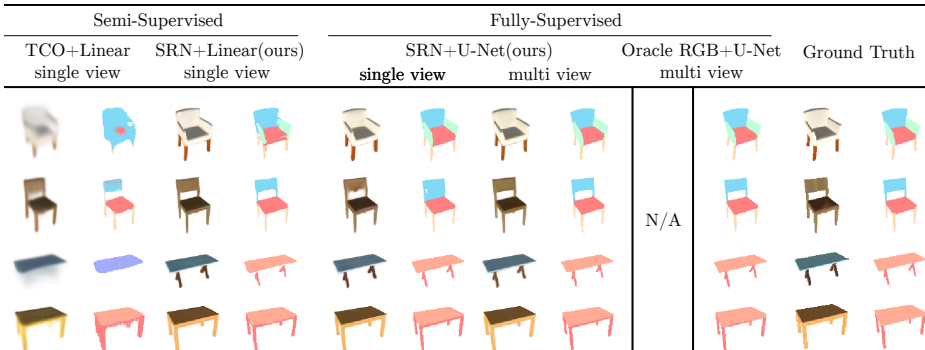


Fig. 4. Qualitative comparison of semi-supervised and fully supervised approaches. *Semi-supervised approaches* (left column) are first pre-trained in an unsupervised manner on a large dataset of posed RGB images. Subsequently, a linear segmentation classifier is fit to a per-pixel feature representation on only *30 pairs of RGB images and their per-pixel semantic labels*. At test time, these methods receive a single posed RGB image. The proposed semi-supervised *SRN+linear* approach succeeds in reconstructing occluded geometry, semantic labels, and appearance, given only a single observation, and far outperforms the baseline 3D representation learning approach by Tatarchenko et al. [60]. *Fully supervised approaches* (center column) are trained on the full training corpus of RGB images and their per-pixel semantic class. At test time, *Oracle RGB+U-Net* receives novel RGB views of the object from an oracle, representing the upper bound of achievable segmentation accuracy. The *SRN+U-Net* baseline first leverages the 3D representation inferred by SRNs for novel view synthesis and segments the resulting image using a 2D U-Net. Here, the SRN representation is inferred from either a *single view* or *multiple views*. This serves as an upper bound for segmentation accuracy if only limited 2D observations are available. Please note that neither of these methods demonstrate a multi-modal 3D representation that encodes information about 3D appearance, geometry, and semantic information, instead performing 2D semantic segmentation in image space. Please see the supplement for semi-supervised *SRN+Linear* multi-shot results.

	Semi-supervised, small dataset		Supervised, small dataset	Supervised, full dataset		
	TCO+linear single view	SRN+linear (ours) single view	Oracle RGB + U-Net single view	SRN+U-Net single view	Oracle RGB + U-Net multi view	Oracle RGB + U-Net multi view
Chairs	28.4 / 23.3	48.7 / 42.3	42.2 / 38.0	60.9 / 51.8	74.2 / 63.7	77.3 / 66.0
Tables	32.8 / 11.4	58.7 / 18.3	50.3 / 17.9	70.8 / 26.5	78.9 / 40.5	81.0 / 44.7

Table 1. Quantitative comparison of semi-supervised and supervised approaches. We benchmark methods on mIOU as well as shape-mIOU. *Semi-supervised* approaches (left column) as well as the *Supervised, small-dataset* baseline are trained on 10 randomly sampled instances, 3 observations each. *Supervised, full dataset* (center column) baselines are trained on all training examples.

semantic classes are present. For each of these instances, we randomly sample 3 posed images. Following the proposed semi-supervised approach, we now freeze the weights of all neural networks and latent codes. We train a simple linear classifier to map features at the intersection points of camera rays with scene geometry to semantic labels.

We benchmark the proposed method with a semi-supervised approach that uses an auto-encoder-based neural scene representation backend, the novel-view synthesis architecture of Tatarchenko et al. [60]. We pre-train this architecture for novel-view synthesis on the full training set to convergence of the validation error and then retrieve features before the last transpose convolutional layer. We then train a single linear transpose convolutional layer on these features on the same subset of labeled examples as the proposed semi-supervised approach for direct comparison.

As a 3D-structure aware reference model, we train the proposed model end-to-end with a U-Net segmentation classifier (see Sec. 3) on the full training dataset. This yields an upper bound of segmentation accuracy of an SRN-based approach in a fully supervised regime of abundant labeled training data. Note that this reference model does *not* infer a compact, multi-modal 3D-aware representation. Instead, this model may perform semantic segmentation in image space, and thus does not come with guarantees that the 3D-aware intermediate representation encodes all information necessary for 3D semantic reasoning.

We first demonstrate that the proposed method enables single-shot reconstruction of a representation that jointly encodes color, geometry, and semantic information. Fig. 3 shows the output of the auto-encoder style baseline, the proposed semi-supervised approach, and the end-to-end trained fully supervised reference model. The proposed semi-supervised approach succeeds in generating a multi-view consistent, dense 3D semantic segmentation, and performs comparable to the end-to-end supervised reference model. Lacking the 3D-structure-aware representation that the proposed model utilizes, the auto-encoder based neural scene representation baseline fails to perform multi-view consistent semantic segmentation. The first four columns of Fig. 4 show further qualitative results for dense 3D semantic segmentation given *single* and *multiple* input views. Finally, Table 1 shows quantitative results for the discussed methods. Consistent with qualitative results, the proposed semi-supervised approach far outperforms the auto-encoder based neural scene representation and even approaches the performance of the single view, fully-supervised SRN reference model (see Table 1, column 4 and Fig. 3). While the proposed model’s linear classifier sometimes struggles with parts of objects with higher inter-instance variance, it performs similarly to the reference models on common parts of objects, such as backrests, legs or the seat in the case of chairs. Thus, the proposed method is the best model in the most difficult regime of single view reconstruction with semi-supervision and is comparable to the performance of the SRN reference model trained in a fully-supervised regime.

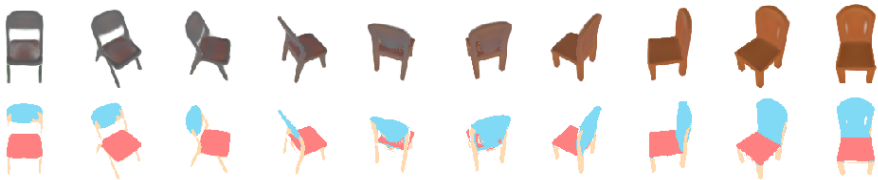


Fig. 5. Interpolating latent code vectors while tracking the camera around the model. Both semantic labels and color features transition smoothly from object to object, demonstrating a tight coupling of semantic labels, geometry and texture of the objects.

4.2 2D reference models with novel-view oracle.

As a reference for how well 2D semantic segmentation algorithms perform on this task, we train a modern U-Net architecture on all pairs of images and their per-pixel semantic labels in the training dataset. This 2D approach does not support predictions about parts of the object that are occluded in the input view. For this reason and to obtain an upper bound for the semantic segmentation performance, at test time, we feed this architecture with a ground-truth RGB rendering of each test view. We note that this is a *significantly* easier task, as these models do not have to perform any 3D reconstruction or, in fact, any 3D reasoning at all, and can instead infer a per-pixel semantic label from 2D pixel neighborhoods with perfect information.

Parameters of the U-Net are approximately matched with the proposed SRN-based approach. Each downsampling layer consists of one stride-one convolutional layer, followed by one stride-two convolutional layer. Each upsampling layer consists of one stride-two transpose convolutional layer, followed by one stride-one convolutional layer. We use BatchNorm and LeakyReLU activations after each convolutional block and dropout with a rate of 0.1. We train this model using the Adam optimizer with a learning rate of $4e-4$ and a batch size of 64 until convergence of validation error after about 80k iterations or 20 epochs.

As expected, this oracle model (Table 1, column 6) outperforms the SRN reference models as well as the proposed semi-supervised method. However, it exists in the easiest regime of all the models, having access to the full dataset of segmentation maps for training and all the oracle RGB views at test time. Qualitatively, for more common objects in the test set, the single-view SRN reference model and the proposed single-view, semi-supervised model actually perform comparably to the oracle model, despite receiving only a small subset of the total information at both train and test time. Furthermore, the proposed models are able to perform the task of generating novel appearance and semantic segmentation views from a single observation, which the 2D-only oracle model cannot even evaluate. However, due to performing 3D reconstruction in addition to semantic segmentation, the proposed method fails whenever 3D reconstruction fails. This may be the case for out-of-distribution objects. This failure mode is completely absent from the 2D oracle method. Please refer to the supplemental video for a detailed investigation of such cases.

For further intuition, we train the reference 2D U-Net on the same 30 image-semantic-label pairs that the proposed semi-supervised approach is trained on. In order to prevent the model from over-fitting, we use the validation set to perform a hyper-parameter search over dropout rates and use early-stopping. Despite using additional segmentation data beyond the 30 training examples in order to perform early-stopping and having access to the RGB novel-view oracle at test time, this U-Net baseline (Tab. 1, column 3) is outperformed by the proposed semi-supervised method. This baseline does not have the compact 3D multi-modal representation of the proposed method, and thus fails to generalize to other instances of the same class nor maintain 3D-consistent views.

4.3 Instance Interpolation.

Interpolating latent vectors inferred in the proposed framework amounts to jointly interpolating geometry, appearance and semantic information. Fig. 5 visualizes a latent-space interpolation of two chairs in the test set, both reconstructed from a single view by the proposed semi-supervised linear model. Geometry, appearance and semantic labels interpolate smoothly, demonstrating a tight coupling of these modalities.

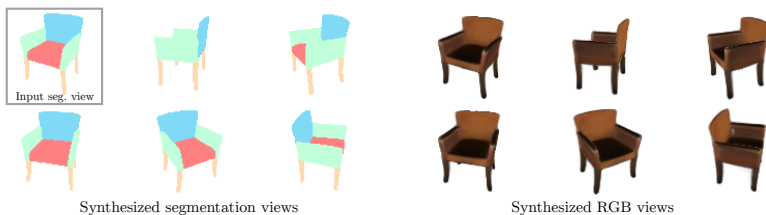


Fig. 6. The proposed representation learning method is bi-directional: it may infer a neural scene representation either from RGB images or semantic segmentation masks, or both. Here, we show renderings of a chair, reconstructed from a single semantic segmentation mask, using the proposed fully supervised model.

4.4 3D reconstruction from semantic mask.

As an instantiation of the auto-decoder framework [46], inferring the neural scene representation of a novel object amounts to initializing and subsequently optimizing a new embedding vector to minimize reconstruction error. As the proposed method may be supervised by both semantic segmentation labels and RGB renderings, it also enables reconstruction of neural scene representations through either modality. Fig. 6 visualizes 3D reconstruction of a chair from a single posed segmentation mask, while Fig. 1 demonstrates reconstruction from a single posed color image.

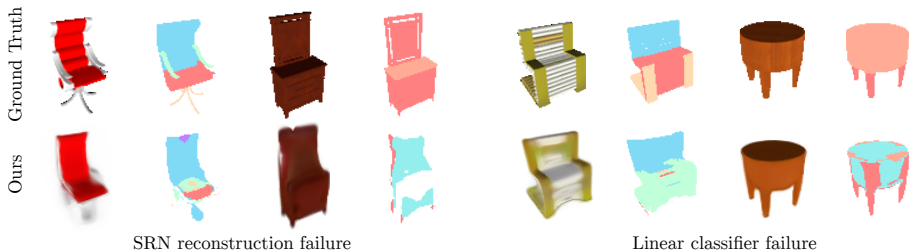


Fig. 7. Failure cases.

4.5 Failure cases.

Fig. 7 displays failure cases of the proposed approach. The proposed approach inherits limitations and failure cases of scene representation networks, such as failure to reconstruct strong out-of-distribution samples or objects with small gaps or high-frequency geometric detail. In these cases, the semantic segmentation fails as well. In the semi-supervised regime, the linear classifier sometimes fails to assign the correct class even if geometry and appearance were reconstructed correctly, which we attribute to its limited representative power. We note that as both appearance-based 3D neural scene representation methods as well as semi-supervised representation learning methods further develop, these failure cases will improve.

5 Discussion

We present a 3D representation learning approach to joint reconstruction of appearance, geometry, and semantic labels. Our semi-supervised approach allows us to perform dense 3D semantic segmentation of a class of objects given as few as 30 human-annotated, posed semantic segmentation masks. At test time, this enables full 3D reconstruction and dense semantic segmentation from either posed RGB images, semantic segmentation masks, or both, from as few as a single observation. After reconstruction, the proposed approach enables multi-view consistent RGB and semantic view generation. We believe that our work outlines an exciting direction of extending representation learning methods into 3D and taking advantage of features that encode both shape and appearance. As both of these fields independently develop more powerful techniques, we expect that our proposed technique, which utilizes these methods collaboratively, will also improve.

Future work may extend the proposed 3D-aware representation learning approach to generalize other scene properties, such as affordance, material properties, mechanical properties, etc. across a class of scenes given extremely few observations. Further, Scene Representation Networks have previously been demonstrated to be capable of reconstructing simple room-scale scenes. We hypothesize that the proposed approach will generalize to such room-scale environments, where it would enable scene semantic segmentation given extremely few labels.

References

1. Achlioptas, P., Diamanti, O., Mitliagkas, I., Guibas, L.: Learning representations and generative models for 3D point clouds. In: Proc. ICML. pp. 40–49 (2018)
2. Bachman, P., Hjelm, R.D., Buchwalter, W.: Learning representations by maximizing mutual information across views. arXiv preprint arXiv:1906.00910 (2019)
3. Chang, A.X., Funkhouser, T., Guibas, L., Hanrahan, P., Huang, Q., Li, Z., Savarese, S., Savva, M., Song, S., Su, H., Xiao, J., Yi, L., Yu, F.: ShapeNet: An Information-Rich 3d Model Repository. arXiv:1512.03012 [cs] (Dec 2015), <http://arxiv.org/abs/1512.03012>, arXiv: 1512.03012
4. Chapelle, O., Scholkopf, B., Zien, Eds., A.: Semi-supervised learning. *IEEE Transactions on Neural Networks* **20**(3), 542–542 (2009)
5. Chen, L.C., Papandreou, G., Kokkinos, I., Murphy, K., Yuille, A.L.: Semantic image segmentation with deep convolutional nets and fully connected crfs. arXiv preprint arXiv:1412.7062 (2014)
6. Choy, C.B., Xu, D., Gwak, J., Chen, K., Savarese, S.: 3d-r2n2: A unified approach for single and multi-view 3d object reconstruction. In: Proc. ECCV (2016)
7. Dai, A., Nießner, M.: 3dmv: Joint 3d-multi-view prediction for 3d semantic scene segmentation. In: Proceedings of the European Conference on Computer Vision (ECCV). pp. 452–468 (2018)
8. Dai, A., Niener, M.: 3dmv: Joint 3d-Multi-View Prediction for 3d Semantic Scene Segmentation. arXiv:1803.10409 [cs] (Mar 2018), <http://arxiv.org/abs/1803.10409>, arXiv: 1803.10409
9. Dai, Z., Yang, Z., Yang, F., Cohen, W.W., Salakhutdinov, R.R.: Good semi-supervised learning that requires a bad gan. In: Advances in neural information processing systems. pp. 6510–6520 (2017)
10. Deng, B., Genova, K., Yazdani, S., Bouaziz, S., Hinton, G., Tagliasacchi, A.: Cvxnets: Learnable convex decomposition. arXiv preprint arXiv:1909.05736 (2019)
11. Doersch, C., Gupta, A., Efros, A.A.: Unsupervised visual representation learning by context prediction. In: Proceedings of the IEEE International Conference on Computer Vision. pp. 1422–1430 (2015)
12. Donahue, J., Krähenbühl, P., Darrell, T.: Adversarial feature learning. arXiv preprint arXiv:1605.09782 (2016)
13. Donahue, J., Simonyan, K.: Large scale adversarial representation learning. arXiv preprint arXiv:1907.02544 (2019)
14. Dosovitskiy, A., Springenberg, J.T., Tatarchenko, M., Brox, T.: Learning to generate chairs, tables and cars with convolutional networks **39**(4), 692–705 (Apr 2017). <https://doi.org/10.1109/TPAMI.2016.2567384>
15. Eslami, S.M.A., Rezende, D.J., Besse, F., Viola, F., Morcos, A.S., Garnelo, M., Ruderman, A., Rusu, A.A., Danihelka, I., Gregor, K., Reichert, D.P., Buesing, L., Weber, T., Vinyals, O., Rosenbaum, D., Rabinowitz, N., King, H., Hillier, C., Botvinick, M., Wierstra, D., Kavukcuoglu, K., Hassabis, D.: Neural scene representation and rendering. *Science* **360**(6394), 1204–1210 (Jun 2018). <https://doi.org/10.1126/science.aar6170>, <https://science.sciencemag.org/content/360/6394/1204>
16. Eslami, S.A., Rezende, D.J., Besse, F., Viola, F., Morcos, A.S., Garnelo, M., Ruderman, A., Rusu, A.A., Danihelka, I., Gregor, K., et al.: Neural scene representation and rendering. *Science* **360**(6394), 1204–1210 (2018)
17. Flynn, J., Broxton, M., Debevec, P., DuVall, M., Fyfe, G., Overbeck, R., Snavely, N., Tucker, R.: DeepView: View synthesis with learned gradient descent. pp. 2367–2376 (Jun 2019)

18. Gadelha, M., Maji, S., Wang, R.: 3d shape induction from 2d views of multiple objects. In: 3DV. pp. 402–411. IEEE Computer Society (2017)
19. Genova, K., Cole, F., Vlasic, D., Sarna, A., Freeman, W.T., Funkhouser, T.: Learning shape templates with structured implicit functions. Proc. ICCV (2019)
20. Groueix, T., Fisher, M., Kim, V.G., Russell, B.C., Aubry, M.: Atlasnet: A papier-mâché approach to learning 3d surface generation. In: Proc. CVPR (2018)
21. Ha, D., Dai, A., Le, Q.V.: Hypernetworks. In: Proc. ICLR (2017)
22. Haene, C., Tulsiani, S., Malik, J.: Hierarchical surface prediction. Proc. PAMI pp. 1–1 (2019)
23. Hénaff, O.J., Razavi, A., Doersch, C., Eslami, S., Oord, A.v.d.: Data-efficient image recognition with contrastive predictive coding. arXiv preprint arXiv:1905.09272 (2019)
24. Hochreiter, S., Schmidhuber, J.: Long short-term memory. Neural Computation **9**(8), 1735–1780 (1997)
25. Jack, D., Pontes, J.K., Sridharan, S., Fookes, C., Shirazi, S., Maire, F., Eriksson, A.: Learning free-form deformations for 3d object reconstruction. CoRR (2018)
26. Jimenez Rezende, D., Eslami, S.M.A., Mohamed, S., Battaglia, P., Jaderberg, M., Heess, N.: Unsupervised learning of 3d structure from images. In: Proc. NIPS (2016)
27. Jing, L., Tian, Y.: Self-supervised visual feature learning with deep neural networks: A survey. arXiv preprint arXiv:1902.06162 (2019)
28. Kanazawa, A., Tulsiani, S., Efros, A.A., Malik, J.: Learning category-specific mesh reconstruction from image collections. In: ECCV (2018)
29. Kar, A., Häne, C., Malik, J.: Learning a multi-view stereo machine. In: Proc. NIPS. pp. 365–376 (2017)
30. Kato, H., Ushiku, Y., Harada, T.: Neural 3d mesh renderer. In: Proc. CVPR. pp. 3907–3916 (2018)
31. Kim, H., Garrido, P., Tewari, A., Xu, W., Thies, J., Niener, M., Prez, P., Richardt, C., Zollhofer, M., Theobalt, C.: Deep video portraits **37**(4), 163:1–14 (Aug 2018). <https://doi.org/10.1145/3197517.3201283>, <https://richardt.name/DeepVideoPortraits/>
32. Kingma, D.P., Mohamed, S., Rezende, D.J., Welling, M.: Semi-supervised learning with deep generative models. In: Advances in neural information processing systems. pp. 3581–3589 (2014)
33. Kumar, A., Eslami, S.A., Rezende, D., Garnelo, M., Viola, F., Lockhart, E., Shananhan, M.: Consistent jumpy predictions for videos and scenes (2018)
34. Larsson, G., Maire, M., Shakhnarovich, G.: Colorization as a proxy task for visual understanding. In: Proceedings of the IEEE Conference on Computer Vision and Pattern Recognition. pp. 6874–6883 (2017)
35. Lombardi, S., Simon, T., Saragih, J., Schwartz, G., Lehrmann, A., Sheikh, Y.: Neural volumes: Learning dynamic renderable volumes from images **38**(4), 65:1–14 (Jul 2019). <https://doi.org/10.1145/3306346.3323020>
36. Long, J., Shelhamer, E., Darrell, T.: Fully convolutional networks for semantic segmentation. In: Proceedings of the IEEE conference on computer vision and pattern recognition. pp. 3431–3440 (2015)
37. Mescheder, L., Oechsle, M., Niemeyer, M., Nowozin, S., Geiger, A.: Occupancy networks: Learning 3d reconstruction in function space. In: Proc. CVPR (2019)
38. Meshry, M., Goldman, D.B., Khamis, S., Hoppe, H., Pandey, R., Snavely, N., Martin-Brualla, R.: Neural Rerendering in the Wild p. 10

39. Mo, K., Zhu, S., Chang, A.X., Yi, L., Tripathi, S., Guibas, L.J., Su, H.: PartNet: A Large-scale Benchmark for Fine-grained and Hierarchical Part-level 3d Object Understanding. arXiv:1812.02713 [cs] (Dec 2018), <http://arxiv.org/abs/1812.02713>, arXiv: 1812.02713
40. Nguyen-Phuoc, T., Li, C., Theis, L., Richardt, C., Yang, Y.L.: HoloGAN: Unsupervised learning of 3D representations from natural images (2019)
41. Nguyen-Phuoc, T., Li, C., Theis, L., Richardt, C., Yang, Y.: Hologan: Unsupervised learning of 3d representations from natural images. In: Proc. ICCV (2019)
42. Nguyen-Phuoc, T.H., Li, C., Balaban, S., Yang, Y.: RenderNet: A deep convolutional network for differentiable rendering from 3d shapes. In: Proc. NIPS (2018)
43. Noroozi, M., Favaro, P.: Unsupervised learning of visual representations by solving jigsaw puzzles. In: European Conference on Computer Vision. pp. 69–84. Springer (2016)
44. Oord, A.v.d., Li, Y., Vinyals, O.: Representation learning with contrastive predictive coding. arXiv preprint arXiv:1807.03748 (2018)
45. Park, J.J., Florence, P., Straub, J., Newcombe, R., Lovegrove, S.: DeepSDF: Learning continuous signed distance functions for shape representation (2019)
46. Park, J.J., Florence, P., Straub, J., Newcombe, R., Lovegrove, S.: DeepSDF: Learning continuous signed distance functions for shape representation. arXiv preprint arXiv:1901.05103 (2019)
47. Qi, C.R., Su, H., Mo, K., Guibas, L.J.: PointNet: Deep Learning on Point Sets for 3d Classification and Segmentation. arXiv:1612.00593 [cs] (Dec 2016), <http://arxiv.org/abs/1612.00593>, arXiv: 1612.00593
48. Qi, C.R., Su, H., Mo, K., Guibas, L.J.: Pointnet: Deep learning on point sets for 3d classification and segmentation. Proc. CVPR (2017)
49. Qi, C.R., Yi, L., Su, H., Guibas, L.J.: PointNet++: Deep Hierarchical Feature Learning on Point Sets in a Metric Space. arXiv:1706.02413 [cs] (Jun 2017), <http://arxiv.org/abs/1706.02413>, arXiv: 1706.02413
50. Qi, C.R., Su, H., Nießner, M., Dai, A., Yan, M., Guibas, L.: Volumetric and multi-view CNNs for object classification on 3d data. In: Proc. CVPR (2016)
51. Radford, A., Metz, L., Chintala, S.: Unsupervised representation learning with deep convolutional generative adversarial networks. arXiv preprint arXiv:1511.06434 (2015)
52. Rasmus, A., Berglund, M., Honkala, M., Valpola, H., Raiko, T.: Semi-supervised learning with ladder networks. In: Advances in neural information processing systems. pp. 3546–3554 (2015)
53. Riegler, G., Ulusoy, A.O., Geiger, A.: Octnet: Learning deep 3d representations at high resolutions. In: Proc. CVPR (2017)
54. Ronneberger, O., Fischer, P., Brox, T.: U-net: Convolutional networks for biomedical image segmentation. In: International Conference on Medical image computing and computer-assisted intervention. pp. 234–241. Springer (2015)
55. Sitzmann, V., Thies, J., Heide, F., Nießner, M., Wetzstein, G., Zollhöfer, M.: DeepVoxels: Learning persistent 3d feature embeddings. In: Proc. CVPR (2019)
56. Sitzmann, V., Thies, J., Heide, F., Niener, M., Wetzstein, G., Zollhfer, M.: DeepVoxels: Learning persistent 3D feature embeddings. pp. 2437–2446 (2019)
57. Sitzmann, V., Zollhfer, M., Wetzstein, G.: Scene Representation Networks: Continuous 3d-Structure-Aware Neural Scene Representations. arXiv:1906.01618 [cs] (Jun 2019), <http://arxiv.org/abs/1906.01618>, arXiv: 1906.01618
58. Srinivasan, P.P., Tucker, R., Barron, J.T., Ramamoorthi, R., Ng, R., Snavely, N.: Pushing the boundaries of view extrapolation with multiplane images. pp. 175–184 (Jun 2019)

59. Sun, X., Wu, J., Zhang, X., Zhang, Z., Zhang, C., Xue, T., Tenenbaum, J.B., Freeman, W.T.: Pix3d: Dataset and methods for single-image 3d shape modeling. In: Proc. CVPR (2018)
60. Tatarchenko, M., Dosovitskiy, A., Brox, T.: Multi-view 3d Models from Single Images with a Convolutional Network. arXiv:1511.06702 [cs] (2015), <http://arxiv.org/abs/1511.06702>
61. Tatarchenko, M., Dosovitskiy, A., Brox, T.: Multi-view 3d models from single images with a convolutional network. In: Proc. ECCV (2016)
62. Tatarchenko, M., Dosovitskiy, A., Brox, T.: Octree generating networks: Efficient convolutional architectures for high-resolution 3d outputs. In: Proc. ICCV. pp. 2107–2115 (2017)
63. Tulsiani, S., Tucker, R., Snavely, N.: Layer-structured 3d scene inference via view synthesis. In: Proc. ECCV (2018)
64. Tulsiani, S., Zhou, T., Efros, A.A., Malik, J.: Multi-view supervision for single-view reconstruction via differentiable ray consistency. In: Proc. CVPR (2017)
65. Tung, H.Y.F., Cheng, R., Fragkiadaki, K.: Learning spatial common sense with geometry-aware recurrent networks. Proc. CVPR (2019)
66. Valentin, J., Vineet, V., Cheng, M.M., Kim, D., Shotton, J., Kohli, P., Nießner, M., Criminisi, A., Izadi, S., Torr, P.: Semanticpaint: Interactive 3d labeling and learning at your fingertips. ACM Transactions on Graphics (TOG) **34**(5), 154 (2015)
67. Vineet, V., Miksik, O., Lidegaard, M., Nießner, M., Golodetz, S., Prisacariu, V.A., Köhler, O., Murray, D.W., Izadi, S., Pérez, P., et al.: Incremental dense semantic stereo fusion for large-scale semantic scene reconstruction. In: 2015 IEEE International Conference on Robotics and Automation (ICRA). pp. 75–82. IEEE (2015)
68. Worrall, D.E., Garbin, S.J., Turmukhambetov, D., Brostow, G.J.: Interpretable transformations with encoder-decoder networks. In: Proc. ICCV. vol. 4 (2017)
69. Wu, J., Zhang, C., Xue, T., Freeman, W.T., Tenenbaum, J.B.: Learning a probabilistic latent space of object shapes via 3d generative-adversarial modeling. In: Proc. NIPS. pp. 82–90 (2016)
70. Wu, Z., Xiong, Y., Yu, S.X., Lin, D.: Unsupervised feature learning via non-parametric instance discrimination. In: Proceedings of the IEEE Conference on Computer Vision and Pattern Recognition. pp. 3733–3742 (2018)
71. Yao, S., Hsu, T.M.H., Zhu, J.Y., Wu, J., Torralba, A., Freeman, W.T., Tenenbaum, J.B.: 3d-Aware Scene Manipulation via Inverse Graphics. arXiv:1808.09351 [cs, eess] (Aug 2018), <http://arxiv.org/abs/1808.09351>, arXiv: 1808.09351
72. Yu, F., Koltun, V.: Multi-scale context aggregation by dilated convolutions. arXiv preprint arXiv:1511.07122 (2015)
73. Zhang, R., Isola, P., Efros, A.A.: Colorful image colorization. In: European conference on computer vision. pp. 649–666. Springer (2016)
74. Zheng, S., Jayasumana, S., Romera-Paredes, B., Vineet, V., Su, Z., Du, D., Huang, C., Torr, P.H.: Conditional random fields as recurrent neural networks. In: Proceedings of the IEEE international conference on computer vision. pp. 1529–1537 (2015)
75. Zhou, T., Tucker, R., Flynn, J., Fyffe, G., Snavely, N.: Stereo magnification: Learning view synthesis using multiplane images **37**(4), 65:1–12 (Aug 2018). <https://doi.org/10.1145/3197517.3201323>
76. Zhou, T., Tucker, R., Flynn, J., Fyffe, G., Snavely, N.: Stereo magnification: learning view synthesis using multiplane images. ACM Trans. Graph. **37**(4), 65:1–65:12 (2018)

77. Zhu, J.Y., Zhang, Z., Zhang, C., Wu, J., Torralba, A., Tenenbaum, J., Freeman, B.: Visual object networks: image generation with disentangled 3d representations. In: Proc. NIPS. pp. 118–129 (2018)
78. Zhu, X., Goldberg, A.B.: Introduction to semi-supervised learning. Synthesis lectures on artificial intelligence and machine learning **3**(1), 1–130 (2009)

Inferring Semantic Information with 3D Neural Scene Representations —Supplement—

Amit Kohli*, Vincent Sitzmann*, and Gordon Wetzstein

Stanford University
{apsk14, sitzmann, gordon.wetzstein}@stanford.edu

1 3D Representation Learning with SRNs [5] Architecture

The basis for our architecture comes from the Scene Representation Network as proposed by Sitzmann et al. [5]. The key insight is that we take the pre-trained features $v \in \mathbb{R}^{256}$ from the neural scene representation and use a simple linear transformation to map those features to class probabilities for each pixel. For an object with c semantic classes, the optimization parameters are a matrix $W \in \mathbb{R}^{256 \times c}$ and bias $b \in \mathbb{R}^c$. Specifically, in the case of chairs $c = 6$ and for tables $c = 11$.

2 Baseline Architecture Tatarchenko et al. [6]

For this baseline we implement the model exactly as specified by Tatarchenko et al. [6]. Implementation information can be found on their github: <https://github.com/lmb-freiburg/mv3d>.

3 UNet Baseline

Here we introduce an additional baseline in order to address the naïve approach of training a 2D to 2D segmentation model on the output of an SRN. This approach has the same input-output capability (single view in, arbitrary appearance and semantic views out) as our proposed model, but does not create a semantically-informed 3D representation and instead infers semantics after rendering images from an existing 3D representation. We demonstrate that the joint representation used by our model allows it to outperform the baseline in a low data regime. In this regime, the baseline overfits very quickly and performs poorly on the test set. Furthermore, because it lacks the 3D structure that is baked into the representation of the proposed model, the baseline tends to fail in classifying difficult views in which key features of the object are occluded. In Fig. 1 we run an experiment training the baseline given increasing amounts of semantically labeled data. For each instance in the variable sized datasets, there

are 3 randomly sampled views per each chair. The models are trained identically with early stopping based on a validation set during training. Each model is then evaluated on the mIOU metric on the test set. It is evident that the baseline’s performance is heavily dependent on the amount of training data. The baseline only matches the performance of our model when it has access to more than 20% of all training instances, whereas our model only requires 0.8% of all training instances. Qualitative comparisons further emphasize this result and can be found in the supplemental video. For this baseline as well as for the oracle models, we use a classic and effective approach for semantic segmentation, a UNet [4]. Specifically, we compare to an architecture based on the one presented in Isola et al. [2], which is shown in Fig. 2.

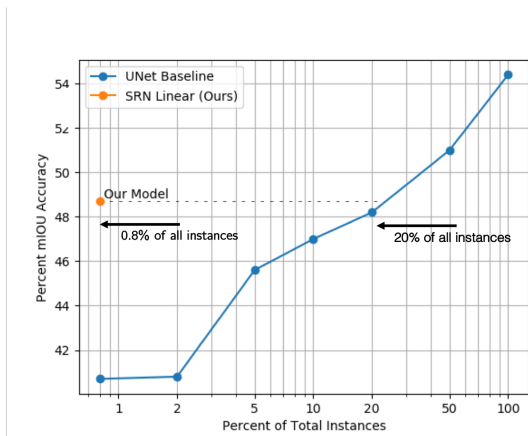


Fig. 1. Graph demonstrating the UNet’s reliance on data for segmentation performance. X-axis is percentage of total instances of objects in the training set, where each instance has 3 random, posed views. Y-axis is the mIOU measure averaged over all test instances. This experiment was performed for the chair object class with a total of 1214 instances.

4 Rendering

For our dataset we use Partnet [3] and Shapenet [1]. For each instance we align a Partnet and Shapenet model and render them using Blender; the Shapenet instance is used for the RGB views and the Partnet instance is used for the corresponding segmentation masks. All camera matrices were also written out in this process. The train-val-test split is from the semantic segmentation task laid out in Mo et al. [3].

5 Baseline Architecture Pix2Pix (Isola et al. [2])

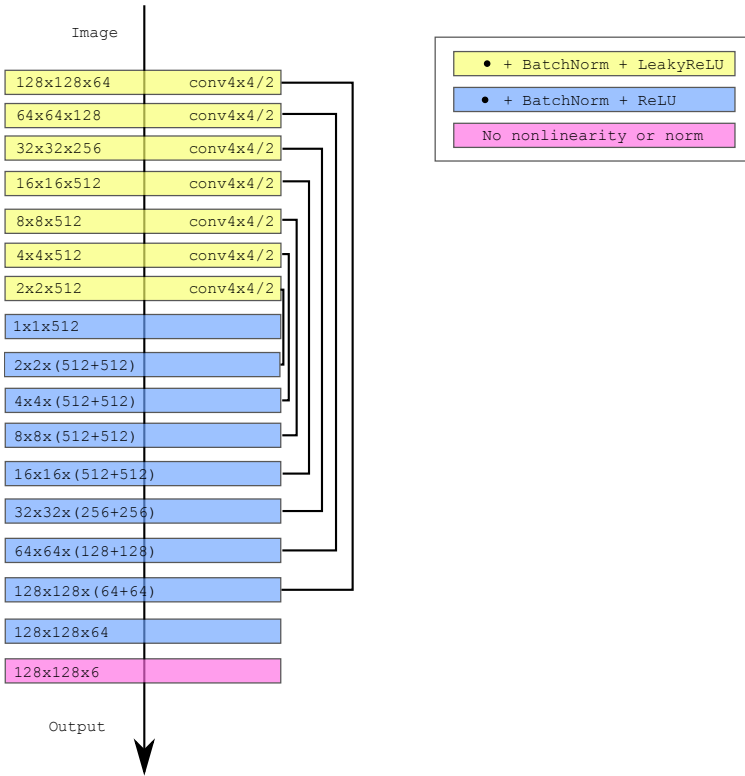


Fig. 2. Architectural details of the image-to-image translation baseline model based on Pix2Pix by Isola et al. [2].

References

1. A. X. Chang, T. Funkhouser, L. Guibas, P. Hanrahan, Q. Huang, Z. Li, S. Savarese, M. Savva, S. Song, H. Su, et al. Shapenet: An information-rich 3d model repository. *arXiv preprint arXiv:1512.03012*, 2015.
2. P. Isola, J.-Y. Zhu, T. Zhou, and A. A. Efros. Image-to-image translation with conditional adversarial networks. In *Proc. CVPR*, pages 5967–5976, 2017.
3. K. Mo, S. Zhu, A. X. Chang, L. Yi, S. Tripathi, L. J. Guibas, and H. Su. Partnet: A large-scale benchmark for fine-grained and hierarchical part-level 3d object understanding. In *Proceedings of the IEEE Conference on Computer Vision and Pattern Recognition*, pages 909–918, 2019.
4. O. Ronneberger, P. Fischer, and T. Brox. U-net: Convolutional networks for biomedical image segmentation. In *International Conference on Medical image computing and computer-assisted intervention*, pages 234–241. Springer, 2015.
5. V. Sitzmann, M. Zollhöfer, and G. Wetzstein. Scene representation networks: Continuous 3d-structure-aware neural scene representations. *CoRR*, abs/1906.01618, 2019.
6. M. Tatarchenko, A. Dosovitskiy, and T. Brox. Single-view to multi-view: Reconstructing unseen views with a convolutional network. *CoRR abs/1511.06702*, 1(2):2, 2015.